Cholesteryl Myristate: Structures of the Crystalline Solid and Mesophases

By **Bryan M. Craven** * and **George T. DeTitta**, Crystallography Department, University of Pittsburgh, Pittsburgh, PA 15260, U.S.A.

Crystals of the title compound are monoclinic, space group $A2$, with lattice parameters a = 10.260(8), b = 7.596(8), c = 101.43(9) Å, β = 94.41(5), and Z = 8 [2 independent molecules (A) and (B)]. The structure was determined from 2 807 observed X-ray intensities, measured by diffractometer. The phase problem was solved by Patterson rotation and translation methods. Refinement by block-diagonal least-squares gave R 0.079. Molecules (A) and (B) have almost fully extended conformations, but differ significantly in the rotation about the ester bond and in the C(17) chains. The crystal structure consists of stacked bilayers 50·7 Å thick. The C(17) chain ends, which lie at the bilayer surfaces, are virtually liquid. Within a bilayer cholesterols pack with cholesterols, and myristate chains pack with myristate chains. The chain packing has an orthorhombic (O_a) subcell. The inner diffraction ring at sin θ/λ 0.015 Å^{-1}, 0.016 Å^{-1} which has been observed for the smectic A and cholesteric mesophases respectively, may be a result of multiple almost parallel 33 Å vectors which exist between atoms of cholesterols on opposite sides of a bilayer. Thus, we infer that the mesophases retain some characteristics of the crystal structure.

THE fatty acid esters of cholesterol have been studied intensively because they form a variety of liquid crystalline phases or mesophases which are intermediate in character between a crystal and an isotropic liquid.[1] These compounds are also of medical importance because they are major components in atherosclerotic lesions. A knowledge of the properties and structures of their crystalline solid phases and mesophases, particularly for those esters involving unsaturated fatty carbon chains, may lead to a better understanding of molecular association in arterial fatty deposits.[2,3] Cholesteric mesophases, so named from the cholesteryl esters, have unusual optical [4] and thermochromic properties which have led to wide technological applications.[5] Structural relationships in crystals [6,7] and in the mesophases [8–13] of the cholesteryl esters have been outlined, but there is a lack of detail. The X-ray scattering from the smectic and cholesteric phases consists of only two diffraction rings [8,12,13] which are difficult to interpret in terms of structural models at the molecular level.[14]

By carrying out the first crystal structure determination of a cholesteryl ester, we have provided new information on which to base extrapolations concerning the structures of the mesophases. The myristate was a convenient choice for initial study because, unlike many other cholesteryl esters, its phase transformations are all reversible: [15]

$$\text{Crystal} \overset{73.6^\circ}{\rightleftharpoons} \text{Smectic A} \overset{79.7^\circ}{\rightleftharpoons} \text{Cholesteric} \overset{85.5^\circ}{\rightleftharpoons} \text{Isotropic liquid}$$

We have also examined the crystal structure of cholesteryl myristate for its possible relevance to the modes of association between cholesterol and the fatty-acid chains within the bilayers of artificial and biological membranes.[16]

EXPERIMENTAL

Cholesteryl myristate was obtained from Sigma Chemical Co. A monoclinic plate-like single crystal (0.20 × 0.50 × 1.00 mm) elongated on b was obtained by slow (6 months) evaporation of an acetone solution at 5 °C. The X-ray data were collected at 25 °C by use of a computer-controlled diffractometer (Picker, FACS 1) and graphite-monochromated Cu-K_α radiation with the crystal mounted so that b^* was inclined at 4.1° from the diffractometer Φ-axis. Lattice parameters were derived by a least-squares fit of angular data for eight reflections with $2\theta > 40°$.

Crystal Data.—$C_{41}H_{72}O_2$, M = 597.1, a = 10.260(8), b = 7.596(8), c = 101.43(9) Å, β = 94.41(5)°, U = 7 881(15) Å^3. D_c = 1.006, Z = 8 (2 molecules in the asymmetric unit), D_m = 1.009 g cm^{-3} (volume dilatometry).[17] Cu-K_α radiation, λ = 1.5418 Å; μ(Cu-K_α) = 4.4 cm^{-1}. Space group $A2$, Am, or $A2/m$ from systematic absences: hkl with $k + l$. However, the space group must be $A2$, since Am and $A2/m$ would require the structure to be racemic.

Barnard and Lydon [7] took single crystal Weissenberg photographs of a series of cholesteryl esters and reported that cholesteryl myristate has space group $P2_1$ with a = 10.18, b = 7.50, c = 50.3 Å, β = 92.5°, and Z = 4. The existence of different crystalline forms of cholesteryl myristate is possible, but unlikely. There have been

[1] G. W. Gray, 'Molecular Structure and the Properties of Liquid Crystals,' Academic Press, London, 1962; G. H. Brown, J. W. Doane, and V. D. Neff, 'A Review of the Structure and Physical Properties of Liquid Crystals,' Chemical Rubber Company Press, Cleveland, Ohio, 1971.
[2] D. M. Small and G. G. Shipley, *Science*, 1974, **185**, 222.
[3] C. W. Griffen and R. S. Porter, *Mol. Cryst. Liq. Cryst.*, 1973, **21**, 77; R. J. Krzewki and R. S. Porter, *ibid.*, p. 99; S. G. Frank and B. G. Byrd, *J. Pharm. Sci.*, 1972, **61**, 1762.
[4] A. DeVries, *Acta Cryst.*, 1951, **4**, 219.
[5] G. H. Brown, *J. Opt. Soc. Amer.*, 1973, **63**, 1505.
[6] J. H. Wendorff and F. P. Price, *Mol. Cryst. Liq. Cryst.*, 1973, **22**, 85.
[7] J. A. W. Barnard and J. E. Lydon, *Mol. Cryst. Liq. Cryst.*, 1974, **26**, 285.
[8] I. G. Chistyakov, *Soviet. Phys. Cryst.*, 1964, **8**, 859.
[9] B. J. Bulkin and K. Krishnan, *J. Amer. Chem. Soc.*, 1971, **93**, 5988.
[10] J. L. W. Pohlmann, W. Elser, and P. R. Boyd, *Mol. Cryst. Liq. Cryst.*, 1971, **13**, 271.
[11] D. Coates and G. W. Gray, *J.C.S. Chem. Comm.*, 1974, 101.
[12] W. L. McMillan, *Phys. Rev. A*, 1972, **6**, 936.
[13] J. H. Wendorff and F. P. Price, *Mol. Cryst. Liq. Cryst.*, 1973, **24**, 129.
[14] A. Guinier, 'X-Ray Diffraction in Crystals, Imperfect Crystals and Amorphous Bodies,' Freeman, San Francisco, 1963, pp. 73, 80; J. Falgueirettes and P. Delord, in 'Liquid Crystals and Plastic Crystals, 2,' eds. G. W. Gray and P. A. Winsor. Wiley, New York, 1974, ch. 3.
[15] E. M. Barrell, R. S. Porter, and J. F. Johnson, *J. Phys. Chem.*, 1966, **70**, 385.
[16] R. P. Rand and V. Luzzati, *Biophys. J.*, 1968, **8**, 125; R. A. Demel, K. R. Bruckdorfer, and L. L. M. van Deenan, *Biochim. Biophys. Acta*, 1972, **255**, 311; D. M. Engelman and J. E. Rothman, *J. Biol. Chem.*, 1972, **247**, 3694; C. H. Huang, J. P. Sipe, S. T. Chow, and R. B. Martin, *Proc. Nat. Acad. Sci. U.S.A.*, 1974, **71**, 359.
[17] F. P. Price and J. H. Wendorff, *J. Phys. Chem.*, 1971, **75**, 2839.

extensive phase equilibrium studies which have revealed crystalline polymorphs of other cholesteryl esters, but not of the myristate.[15] The discrepancy between the two unit cells may not be real. Initially, we obtained dimensions for a subcell very similar to those of Barnard and Lydon when we misinterpreted our own Weissenberg photographs. The indexing of $\bar{1}02$ as 100 and 002 as 001 gave $a = 10.23$, $c = 50.6$, and $\beta = 91.4°$. Because the c^* axis is so much shorter than the other reciprocal axes, we discovered the spectral absences for $k + l$ odd in an $0kl$ photograph only after accurate diffractometer measurements had led us to a correct unit cell.

X-Ray intensity data for cholesteryl myristate were collected in two batches. First, the 901 reflections with $2\theta < 50°$ were measured with $\theta : 2\theta$ scans at a rate of 2° min^{-1} in 2θ, using a variable scan-width based on 1.6°. Then, 4 795 reflections with $50° < 2\theta < 100°$ were measured with ω scans at a rate of 1° min^{-1}, using variable scan-widths with a base-width of 1.4°. The ω scans were used for the higher Bragg angles in order to optimize the resolution of neighbouring reciprocal lattice points. Data collection did not extend beyond 2θ 100° because there were few significant intensities at higher angles. Thus, in the range $88° < 2\theta < 100°$ there were only 343 out of a total of 1 213 reflections for which the integrated intensity, I, was $> 2\sigma(I)$. The data subsets were scaled so as to equalize the sums of the intensities of 51 reflections which were measured by both scan techniques.

The number of intensities was reduced to 4 599 by averaging over symmetry-related reflections and by omitting reflections with $|l| \geq 100$ (for convenience in data processing). Data were not corrected for *X*-ray absorption or extinction.

A Laue diffraction camera was constructed for the study of powdered crystal and liquid crystalline phases. The sample holder consisted of a pair of beryllium windows cut from the casing of a discarded *X*-ray tube, separated by a Teflon washer to form a cavity for the sample of thickness 1 mm. The sample was electrically heated, the temperature being measured by a thermocouple embedded in the sample holder. For thermal insulation, this assembly was enclosed in the top section of another old *X*-ray tube so that incident and scattered *X*-ray beams could be passed through opposite beryllium windows. This gave a maximum observed scattering angle of 20°. For satisfactory resolution in the low-angle scattering region, the incident Ni-filtered Cu-K_α *X*-rays were collimated by means of pinholes 13 in apart. The sample to flat-plate film-holder distance was 6 in. Our *X*-ray photographs of cholesteryl myristate smectic, cholesteric, and isotropic liquid phases, confirm previously reported results [12,13] except for the apparent errors in 2θ values shown by Wendorff and Price [13] in their Figures 1 and 2. Each mesophase gave only two diffraction rings with uniform intensities around the rings. For the smectic phase, at 72 ± 2 °C (14 h *X*-ray exposure) the intense sharp inner ring was at 2θ 2.67° or $\sin\theta/\lambda$ 0.015 $Å^{-1}$ and the very weak diffuse outer ring peaked at *ca.* 2θ 17.6° or $\sin\theta/\lambda$ 0.099 $Å^{-1}$. The inner ring was almost as sharp as the 002 and 004 powder diffraction rings which occur at $\sin\theta/\lambda$ 0.010 $Å^{-1}$ and 0.020 $Å^{-1}$ respectively. For the cholesteric phase at 82 °C, the inner ring was less intense and more diffuse and it occurred at a slightly higher angle ($\sin\theta/\lambda$ 0.016 $Å^{-1}$). For the isotropic liquid (100 °C) the inner ring was very weak and so diffuse that it was not clearly resolved from the direct *X*-ray beam. There were no recognizable changes in the outer diffraction rings in these photographs. The broad outer ring corresponded to a region of intense powder diffraction due to side-spacings in the crystal structure.

Crystal Structure Determination.—The sharpened Patterson function calculated with quasinormalized E^2 coefficients was found to be dominated by peaks which were consistent with close packing of extended hydrocarbon chains running approximately parallel to the [$\bar{2}01$] direction. The packing of the complete structure was almost correctly deduced with the aid of molecular models, but no trial structure could be found which gave R better than 0.45.

The phase problem was finally solved by the use of Patterson rotation and translation function methods. For this purpose, a linked sequence of computer programs was written [18] which incorporated the fast rotation routines by Crowther,[19] and the translation function suggested by Langs.[20] The latter is given by

$$\Phi(X,Y,Z) = \sum_h G(h)\cos[2\pi(hX + kY + lZ) - (\phi_j - \phi_i)]$$

where

$$G(h) = |E(h)_o|^2 - \sum_{n=1}^{N} |E(h)_n|^2.$$

The $|E(h)_n|$ and ϕ_n are the calculated quasinormalized structure amplitude and phase for the n^{th} of a total of N rigid-body structural fragments. Each $|E(h)_n|$ and ϕ_n are calculated for a properly oriented fragment with an arbitrarily chosen fragment origin. The value of $\Phi(X,Y,Z)$ should peak at the vector separation between a selected pair (i^{th} to the j^{th}) of these local origins.

The rotation function was used to match the Patterson function of cholesteryl myristate with that of a rotated artificial crystal structure composed of a nineteen-atom cholesterol fragment. Atomic co-ordinates for the cholesterol ring system were derived from the crystal structure of 3β-chloroandrost-5-en-17β-ol.[21] In the asymmetric volume of rotation space, the six highest peaks had relative magnitudes 225, 217, 184, 182, 177, and 177, with the next-highest peaking at 96. The two largest peaks were taken as giving the orientations of the two crystallographically independent cholesterol fragments [(A) and (B)] in cholesteryl myristate. The next four peaks, which differed by multiple rotations of almost 60° from the two largest peaks, were consistent with the pseudosymmetry of the cholesterol ring system.

Three Φ syntheses were then calculated to search for the relative translations of pairs of cholesterol fragments in the crystal structure, namely a pair of (A) and a pair of (B) fragments which must each be related by crystallographic two-fold axes, and thirdly an (A)–(B) pair. Although the Φ maps contained spurious features, there was no difficulty in selecting a large peak from each which formed a consistent set of vectors between fragment origins. In this way, both cholesterol fragments (A) and (B) were correctly positioned. In the subsequent search for the myristate chains, four cholesterol fragments [two (A) and two (B)] were combined

[18] B. M. Craven, ' Computer Programs ROTRAN,' Technical Report, Crystallography Department, University of Pittsburgh.
[19] R. A. Crowther, in ' The Molecular Replacement Method,' ed. M. G. Rossman, *Internat. Sci. Rev.*, 1973, **13**, 171.
[20] D. A. Langs, *Acta Cryst.*, 1975, **A31**, 543.
[21] C. M. Weeks, A. Cooper, and D. H. Norton, *Acta Cryst.* 1971, **B27**, 531.

to form a superfragment with an origin located on a crystallographic two-fold axis. The chain search-fragment consisted of a planar 12-atom zig-zag with bond lengths of 1.53 Å, bond angles of 112°, and an orientation determined by inspection of the cholesteryl myristate Patterson function. A Φ-map gave two large peaks which positioned the chains so that they could be connected by ester linkages to each cholesterol fragment.

The resulting structure, which was complete except for the chains at C(17), gave a molecular packing arrangement with no atoms closer than the usual van der Waals distances. Structure-factor calculations with 70 of the total 86 carbon and oxygen atoms gave R 0.41. After three cycles of Fourier syntheses and structure-factor calculations, the remaining atoms were located, although positions for the terminal atoms C(25)—(27) for each molecule remained doubtful; R was 0.31.

Refinement was carried out by a block-diagonal least-squares procedure so as to minimize $\sum_h w_h\{|F(h)_o|^2 - |F(h)_c|^2\}$ where the weights w_h were assigned to be $\{10.0 + 0.008|F(h)|^2\}^{-\frac{1}{2}}$. Damping factors of 0.5 and 0.2 were applied to the changes in atomic positional and thermal parameters respectively. The 1 792 reflections with $I < 2\ \sigma(I)$ were excluded so as to reduce computing time. Atomic scattering factors of ref. 22 were used for carbon and oxygen. After two cycles (R 0.26), a Fourier synthesis was calculated, which indicated revised configurations for atoms C(25)—(27).

At this stage the positions for 126 of the hydrogen atoms were calculated at standard bonding distances (1.0 Å) and angles from the carbon atom framework. Hydrogen atoms bonded to atoms C(24)—(27) were omitted because of the large thermal amplitudes of vibration in this region of the structure. Hydrogen atoms were included in structure-factor calculations with isotropic temperature factors assumed to be the same as for the carbon atoms to which they are bonded. Hydrogen atom parameters were not subsequently refined. The atomic scattering factor for hydrogen was from ref. 23. The nature of the crystal structure led to unexpectedly high hydrogen-atom contri-

[22] D. T. Cromer and J. T. Waber, *Acta Cryst.*, 1965, **18**, 104.
[23] R. F. Stewart, E. R. Davidson, and W. T. Simpson, *J. Chem. Phys.*, 1965, **42**, 3175.

TABLE 1

Positional parameters (x,y,z) as fractional co-ordinates multiplied. The transformation $X = 9.880x + 19.760z$; $Y = 7.60y$; $Z = -2.766x + 99.456z$ gives atomic Cartesian co-ordinates in Å units, with the Z axis along [$\bar{2}$01] which is almost parellel to the molecular long axes. Anisotropic thermal parameters are given according to the expression: $T = \exp[-\sum_i\sum_j \beta_{ij}h_ih_j]$. Estimated standard deviations are in parentheses

(*a*) Molecule (A)

Atom	$x(10^4)$	$y(10^4)$	$z(10^5)$	$\beta_{11}(10^4)$	$\beta_{22}(10^3)$	$\beta_{33}(10^5)$	$\beta_{12}(10^3)$	$\beta_{13}(10^5)$	$\beta_{23}(10^5)$
O	4 302(7)	5 873(14)	16 281(7)	143(10)	41(3)	15(1)	6(2)	11(8)	41(15)
O(3)	6 392(7)	4 917(12)	16 258(7)	125(9)	26(2)	12(1)	1(1)	7(7)	18(12)
C(1)	6 834(11)	7 000(13)	12 962(10)	155(15)	7(2)	13(1)	−1(2)	12(11)	−3(14)
C(2)	6 707(10)	6 912(16)	14 448(10)	114(14)	19(3)	12(1)	−0(2)	17(11)	5(15)
C(3)	6 355(10)	5 014(16)	14 821(9)	131(14)	22(3)	9(1)	0(1)	−8(10)	−21(16)
C(4)	7 373(12)	3 764(17)	14 377(11)	191(19)	20(3)	14(2)	6(2)	46(14)	32(18)
C(5)	7 669(10)	3 937(16)	13 028(9)	117(13)	20(3)	8(1)	0(2)	15(9)	−4(15)
C(6)	7 653(11)	2 523(14)	12 225(10)	164(16)	10(2)	11(1)	0(2)	0(12)	45(15)
C(7)	8 031(12)	2 497(15)	10 845(11)	159(16)	12(3)	16(2)	4(2)	18(13)	40(17)
C(8)	8 566(10)	4 255(14)	10 358(10)	86(12)	13(2)	14(1)	2(2)	44(10)	−5(15)
C(9)	7 798(9)	5 763(14)	10 991(9)	81(11)	12(2)	9(1)	0(1)	−5(8)	−40(13)
C(10)	7 903(9)	5 770(13)	12 460(13)	97(12)	9(2)	12(1)	0(1)	−7(9)	2(15)
C(11)	8 146(11)	7 565(14)	10 345(10)	163(16)	10(2)	13(1)	4(2)	37(12)	45(15)
C(12)	8 190(10)	7 559(13)	8 858(9)	154(15)	7(2)	11(1)	2(2)	9(11)	1(14)
C(13)	9 079(9)	6 129(13)	8 367(9)	132(13)	5(2)	11(1)	−4(1)	3(10)	−34(14)
C(14)	8 538(10)	4 400(13)	8 900(10)	112(13)	10(2)	13(1)	0(1)	−3(10)	−19(14)
C(15)	9 242(13)	3 013(18)	8 188(11)	213(19)	18(3)	13(1)	2(2)	9(14)	33(18)
C(16)	9 389(12)	3 804(18)	6 826(12)	160(17)	23(3)	19(2)	8(2)	15(14)	−46(20)
C(17)	8 931(10)	5 714(13)	6 898(9)	125(14)	9(2)	11(1)	1(2)	−11(10)	−34(14)
C(18)	10 452(11)	6 472(17)	8 910(11)	138(15)	21(3)	17(2)	−7(2)	−7(12)	−20(19)
C(19)	9 231(11)	6 381(18)	13 065(10)	137(15)	25(3)	14(1)	−5(2)	18(11)	−10(19)
C(20)	9 769(12)	6 847(15)	5 938(12)	209(19)	12(2)	16(2)	2(2)	35(14)	−51(17)
C(21)	9 467(13)	8 827(17)	6 072(11)	242(21)	19(3)	13(1)	−2(2)	42(14)	8(18)
C(22)	9 483(16)	6 311(21)	4 522(12)	384(29)	23(3)	16(2)	4(3)	49(18)	59(22)
C(23)	10 406(24)	7 010(31)	3 520(18)	632(50)	49(7)	23(3)	16(5)	212(31)	183(35)
C(24)	11 598(21)	6 295(48)	3 595(24)	312(32)	95(12)	49(4)	14(6)	151(31)	21(72)
C(25)	12 510(24)	7 276(95)	2 426(22)	362(45)	403(46)	26(4)	21(13)	34(32)	−110(98)
C(26)	13 590(24)	5 966(82)	2 616(25)	351(42)	254(34)	45(5)	−17(11)	204(36)	−348(97)
C(27)	11 965(39)	6 827(99)	1 639(42)	580(82)	231(42)	91(11)	20(18)	−21(77)	47(99)
C(28)	5 292(11)	5 351(15)	16 863(10)	166(17)	16(2)	12(1)	−3(2)	8(12)	11(15)
C(29)	5 553(12)	5 210(20)	18 322(11)	180(18)	32(2)	11(1)	−1(2)	18(12)	59(19)
C(30)	4 544(11)	5 808(17)	19 171(10)	175(16)	20(3)	10(1)	−3(2)	15(11)	−9(17)
C(31)	4 912(10)	5 461(17)	20 625(11)	88(13)	25(3)	16(2)	−2(2)	8(11)	22(18)
C(32)	3 992(10)	6 091(16)	21 600(10)	141(15)	16(2)	15(1)	2(2)	22(11)	17(18)
C(33)	4 420(11)	5 649(17)	23 002(10)	174(17)	22(3)	11(1)	−3(12)	13(12)	62(17)
C(34)	3 503(12)	6 150(19)	24 033(10)	190(17)	23(3)	12(1)	3(2)	−9(12)	0(19)
C(35)	3 986(10)	5 628(16)	25 429(10)	116(13)	19(3)	13(1)	−1(2)	14(11)	10(16)
C(36)	3 065(10)	6 091(16)	26 458(10)	122(14)	17(2)	14(1)	−2(2)	16(11)	−16(18)
C(37)	3 514(11)	5 530(17)	27 853(10)	150(15)	22(3)	12(1)	0(2)	−11(12)	7(17)
C(38)	2 623(11)	5 997(18)	28 905(10)	157(15)	22(3)	13(1)	3(2)	26(12)	−43(20)
C(39)	3 028(11)	5 342(17)	30 280(10)	156(16)	23(3)	13(1)	1(2)	24(12)	3(17)
C(40)	2 133(11)	5 861(19)	31 308(11)	149(16)	24(3)	16(2)	−2(2)	41(13)	−36(21)
C(41)	2 533(15)	5 096(24)	32 688(12)	250(23)	41(5)	14(2)	−3(3)	50(16)	−44(24)

TABLE 1 (*Continued*)

(*b*) Molecule (B)

Atom	$x(10^4)$	$y(10^4)$	$z(10^5)$	$\beta_{11}(10^4)$	$\beta_{22}(10^3)$	$\beta_{33}(10^5)$	$\beta_{12}(10^3)$	$\beta_{13}(10^5)$	$\beta_{23}(10^5)$
O	4 025(7)	1 234(18)	17 584(7)	135(10)	64(4)	12(1)	−5(2)	7(8)	20(18)
O(3)	2 212(7)	1 067(14)	16 299(7)	134(10)	38(3)	15(1)	−4(2)	10(8)	3(15)
C(1)	3 612(10)	−357(17)	13 147(11)	155(15)	18(3)	14(1)	3(2)	32(12)	44(17)
C(2)	2 958(12)	−566(19)	14 433(13)	171(18)	24(3)	18(2)	2(2)	−3(14)	90(21)
C(3)	2 897(10)	1 260(20)	15 085(10)	109(13)	34(3)	11(1)	−4(2)	3(10)	15(20)
C(4)	2 213(10)	2 548(18)	14 181(11)	111(14)	24(3)	14(1)	2(2)	30(12)	−39(19)
C(5)	2 744(9)	2 662(15)	12 850(10)	71(11)	17(2)	13(1)	0(2)	−25(10)	5(16)
C(6)	3 058(11)	4 203(16)	12 354(11)	157(16)	17(3)	14(1)	1(2)	36(12)	−28(17)
C(7)	3 547(10)	4 490(14)	11 049(11)	123(15)	8(2)	20(2)	−2(2)	9(13)	−18(16)
C(8)	3 382(9)	2 859(14)	10 148(9)	90(12)	12(2)	12(1)	1(2)	−22(10)	16(15)
C(9)	3 788(10)	1 177(16)	10 951(9)	118(13)	16(2)	11(1)	3(2)	−6(10)	6(16)
C(10)	2 883(9)	967(14)	12 135(9)	106(12)	10(2)	9(1)	0(2)	−32(9)	5(14)
C(11)	3 865(12)	−474(15)	10 069(11)	192(18)	8(2)	16(2)	2(2)	22(13)	−19(15)
C(12)	4 464(11)	−131(15)	8 878(10)	153(15)	9(2)	12(1)	2(2)	6(11)	−16(15)
C(13)	4 120(9)	1 388(16)	8 021(9)	90(12)	20(3)	10(1)	−2(2)	17(9)	0(15)
C(14)	4 202(10)	2 998(15)	9 002(10)	118(14)	14(2)	11(1)	−1(2)	−35(10)	28(15)
C(15)	4 008(12)	4 606(17)	8 019(12)	162(16)	13(3)	19(2)	1(2)	15(14)	88(18)
C(16)	4 642(13)	3 977(18)	6 814(13)	185(18)	18(3)	21(2)	3(2)	89(15)	0(21)
C(17)	4 987(10)	2 049(16)	6 995(10)	111(13)	21(3)	11(1)	0(2)	−7(11)	−19(16)
C(18)	2 765(10)	1 024(19)	7 448(10)	116(14)	28(3)	13(1)	−4(2)	−4(2)	−46(20)
C(19)	1 576(11)	264(17)	11 669(16)	163(16)	23(3)	8(1)	−7(2)	−10(11)	19(16)
C(20)	5 008(11)	1 065(20)	5 675(10)	157(16)	26(3)	12(1)	−3(2)	20(12)	31(20)
C(21)	5 296(15)	−928(25)	5 791(14)	243(24)	39(5)	20(2)	−4(3)	54(18)	3(28)
C(22)	5 993(15)	1 855(22)	4 936(14)	233(22)	31(4)	22(2)	6(3)	4(17)	26(24)
C(23)	6 054(18)	1 310(33)	3 379(16)	333(31)	57(7)	21(2)	−4(4)	79(22)	−6(37)
C(24)	7 137(22)	2 179(18)	2 718(19)	458(41)	73(10)	27(3)	−18(6)	196(28)	−12(43)
C(25)	7 324(25)	1 020(81)	1 506(24)	418(49)	280(33)	40(4)	27(12)	252(38)	468(119)
C(26)	8 564(29)	1 523(96)	1 332(38)	357(50)	314(51)	82(9)	16(15)	151(59)	−619(207)
C(27)	7 047(68)	2 382(98)	828(40)	1 975(272)	281(52)	57(9)	159(34)	183(98)	482(172)
C(28)	2 895(11)	1 028(17)	17 463(10)	156(15)	17(3)	11(1)	3(2)	−12(11)	30(18)
C(29)	2 047(11)	582(18)	18 534(11)	141(16)	26(3)	14(1)	−6(2)	27(12)	−5(19)
C(30)	2 576(12)	1 067(19)	19 887(11)	194(18)	20(3)	15(2)	−2(2)	−33(13)	35(20)
C(31)	1 697(11)	631(18)	20 949(11)	135(15)	26(3)	14(1)	3(2)	−14(12)	38(19)
C(32)	2 198(11)	1 062(18)	22 340(9)	159(15)	25(3)	8(1)	−3(2)	−5(11)	23(18)
C(33)	1 256(11)	648(19)	23 378(11)	143(16)	27(3)	13(1)	3(2)	5(12)	−1(19)
C(34)	1 738(11)	1 097(20)	24 772(10)	157(16)	27(3)	12(1)	2(2)	−32(12)	−25(20)
C(35)	796(11)	625(18)	25 800(10)	122(14)	28(3)	11(1)	−6(2)	3(11)	−21(18)
C(36)	1 233(11)	1 033(17)	27 191(10)	155(15)	20(3)	12(1)	2(2)	−4(12)	−26(19)
C(37)	278(10)	607(17)	28 212(9)	128(14)	27(3)	9(1)	3(2)	2(10)	−4(17)
C(38)	706(11)	1 003(21)	29 623(10)	128(14)	33(4)	13(1)	1(2)	−10(11)	3(21)
C(39)	−228(11)	598(20)	30 624(11)	116(14)	39(4)	13(1)	−4(2)	20(11)	0(21)
C(40)	170(11)	985(23)	32 064(12)	128(16)	42(4)	16(2)	2(3)	0(12)	−49(26)
C(41)	−790(14)	681(27)	33 035(11)	200(20)	58(6)	12(1)	−10(3)	17(14)	−6(26)

butions for many reflections, so that inclusion of the hydrogen scattering is believed to have had a significant effect on the final values of the heavier-atom parameters. Thus, for the strong reflection $3,1,\overline{37}$ with $|F_o|$ 197, $|E_o|$ 3.43, and sin $\theta/\lambda = 0.23$ Å^{-1}, the total hydrogen scattering amplitude was 63.

With R 0.15, anisotropic temperature factors were introduced. After another eight cycles in which 795 parameters were varied, the refinement was discontinued, although in the final cycle there were still nineteen x or z parameters which changed by $>0.5\ \sigma$ or 0.005 Å.* The final R value was 0.079. Final atomic parameters are listed in Table 1.†

RESULTS

Description of the Structure.—Mean values of the bond angles and distances in the two crystallographically independent molecules are shown in Figure 1. The root-mean-square differences between observed and mean values, excluding those for the terminal isopropyl groups, are 0.015 Å for the bond lengths and 1.2° for bond angles. These are considered to be more reliable error estimates than the corresponding estimated standard deviations from the least-squares procedure (0.014 Å and 0.9°). For the tetracyclic system, the bond lengths and angles are not significantly different from those in the molecule of 3β-chloroandrost-5-en-17β-ol,[21] which served as a search model in the present structure determination. The bond lengths and angles in the terminal isopropyl groups of cholesteryl myristate are not physically meaningful because of the unusually high atomic thermal motions. The maximum principal values of the root-mean-square thermal amplitudes for these atoms range from 0.8 to 1.3 Å. From the thermal ellipsoids shown in Figure 2, drawn at the 50% probability level, and from the correspondingly very diffuse peaks observed in the electron-density distribution, we suggest that the isopropyl ends of both molecules are virtually in the liquid state.

Bond lengths and angles in the myristate chains appear to be significantly and systematically different from the expected values of 1.53 Å and 112°.[24] This effect could arise from a thermal libration of each chain about its chain axis. A librational amplitude of 20°, which would require

* In the block-diagonal refinement procedure, the y parameters were refined for all carbon and oxygen atoms. Although the origin was 'fixed' in the b direction by means of the fixed hydrogen-atom configuration, there were small but significant translations of the structure along b during the refinement.

† Observed and calculated structure amplitudes and the assumed hydrogen atom parameters are listed in Supplementary Publication No. SUP 21645 (24 pp., 1 microfiche). For details see Notice to Authors No. 7, in *J.C.S. Perkin II*, 1975, Index issue.

[24] D. R. Lide, *Tetrahedron*, 1962, **17**, 125; L. H. Jensen and A. J. Mabis, *Acta Cryst.*, 1966, **21**, 770.

atomic displacements of 0.15 Å normal to the plane of the chain, would be consistent with the observed minimum principal root-mean-square amplitude for a chain atom [0.19 Å for atom C(33)]. This is an oversimplified model for the thermal motion of the chains. Nevertheless, assuming a rigid chain with bond lengths and angles of 1.530 Å and 112°,

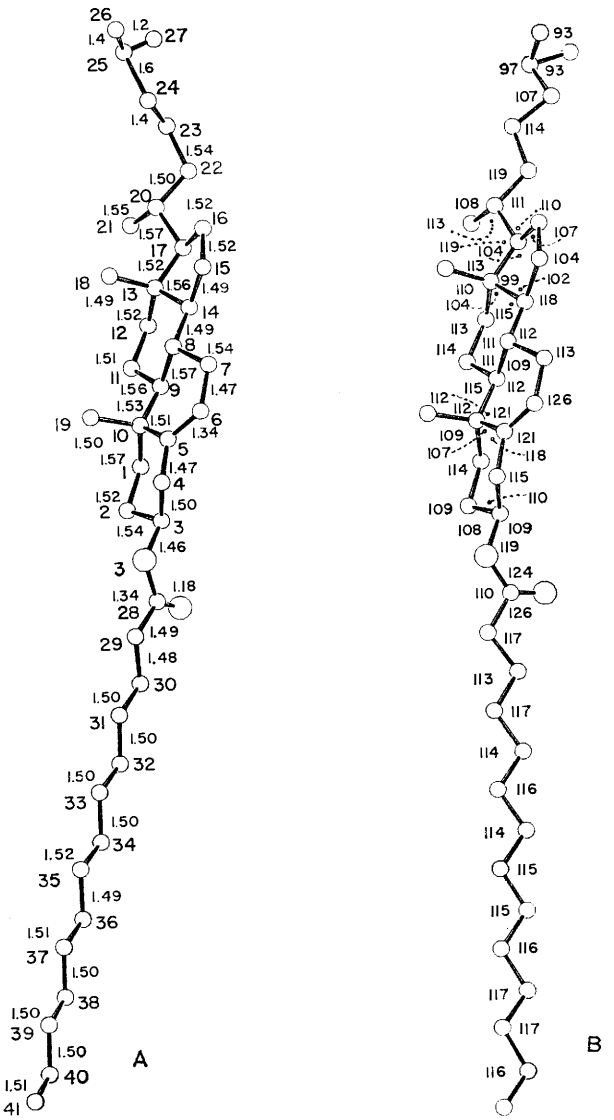

FIGURE 1 Atomic numbering system, mean bond lengths (Å) and angles (°) for cholesteryl myristate, molecules (A) and (B), shown in their observed configurations with the tetracyclic ring systems in the same orientation

to have a 20° libration of this kind, the lengths and angles involving atomic thermal centroids would be 1.50 Å and 115°, which is in agreement with the observed mean values.

There are considerable differences in the conformations of molecules (A) and (B), but not in the tetracyclic system. The superposability of the C(1)—(19) fragments of the two molecules was estimated by means of a best least-squares fit.[25] The resulting root-mean-square displacement of corresponding atoms was 0.054 Å. There were also good fits to the C(1)—(19) fragment from 3β-chloroandrost-5-en-17β-ol which was used in the Patterson search. Root-mean-square atomic displacements were 0.076 Å for the fit to molecule (A) and 0.050 Å for molecule (B).*

Table 2 lists best least-squares planes through selected atoms in each molecule. In each of the ester linkages and

TABLE 2

Best least-squares planes. The calculated planes are as follows: (1) cholesteryl ring system, atoms C(1)—(17); (2) central section of the myristate chain, atoms C(32)—37); (3) ester group, O(3), C(28), O, C(29); and (4) ethylenic group C(5), C(6), C(4), C(10), C(7). Equations are in the form: $ax + by + cz = d$, referred to the crystal axes, with plane constants in Å

(*a*) Plane constants, values for molecule (A) above those for molecule (B)

Plane	*a*	*b*	*c*	*d*
(1)	9.439	1.014	30.091	11.357
	9.504	1.190	27.424	6.647
(2)	4.619	6.715	9.525	8.019
	4.037	−6.941	7.600	1.839
(3)	3.280	7.189	3.110	6.130
	−1.745	7.420	14.833	2.829
(4)	9.801	−0.779	20.596	9.876
	9.272	−0.699	35.229	6.880

(*b*) Distances (Å) of atoms from the planes. Values for molecule (A) precede those for molecule (B)

Plane (2): C(32) −0.03, 0.01; C(33) 0.01, −0.01; C(34) 0.02, −0.02; C(35) 0.02, 0.01; C(36) 0.01, 0.01; C(37) −0.03, 0.00; C(28) * −0.38, −0.06; C(29) * −0.21, −0.01; C(30) * −0.19, −0.03; C(31) * −0.12, 0.00; C(38) * −0.03, 0.00; C(39) * −0.15, −0.02; C(40) * −0.12, −0.02; C(41) * −0.31, −0.12

Plane (3): O 0.01, −0.01; O(3) 0.01, −0.01; C(28) −0.02, 0.02; C(29) 0.01, −0.01; C(3) * 0.02, −0.16; C(30) * 0.13, 0.46

Plane (4): C(10) −0.01, 0.00; C(5) 0.02, 0.01; C(4) 0.02, −0.01; C(6) −0.05, 0.01; C(7) 0.03, −0.01

* Atom not included in derivation of plane.

around the C(5)=C(6) ethylenic groups, the atoms are nearly coplanar.

Conformational differences in molecules (A) and (B) lead to large relative displacements at both ends of the molecule when the tetracyclic systems are superposed. Atoms C(40) and C(41) at the myristate end are displaced by 3.9 and 3.6 Å respectively, atoms C(24) and C(25) by 2.6 and 2.9 Å.

The myristate chains are both almost fully extended (Figures 1, 2, 3b) although there is a slight bowing which is more pronounced in chain (A) (Table 2, Figure 3b). Molecules (A) and (B) are related by a bodily movement of the myristate chains with respect to the cholesterol portion, due to differences in rotation about the ester bond C(3)–O(3). In molecule (B), the torsion angles C(4)–C(3)–O(3)–C(28) and C(2)–C(3)–O(3)–C(28) are −136.0 and 102.2°. The carbonyl bond more nearly eclipses the C(3)–H bond than in molecule (A), where the corresponding torsion angles are −154.9 and 87.0°. In molecule (A), the carbonyl oxygen atom is closer to C(2), with an intramolecular O · · · C distance of 3.30 Å, *vs.* 3.57 Å in molecule (B). The dihedral angle between the best least-squares planes through the atoms of the cholesterol rings and through the myristate

* The accuracy of the assumed search fragment undoubtedly contributed to the success of the crystal structure determination, although there were significant errors in the initial atomic positions obtained from the rotational and translational search. These errors were greatest for molecule (B) in which six atoms were *ca.* 0.3 Å from their final refined positions.

[25] S. C. Nyburg, *Acta Cryst.*, 1974, **B30**, 251.

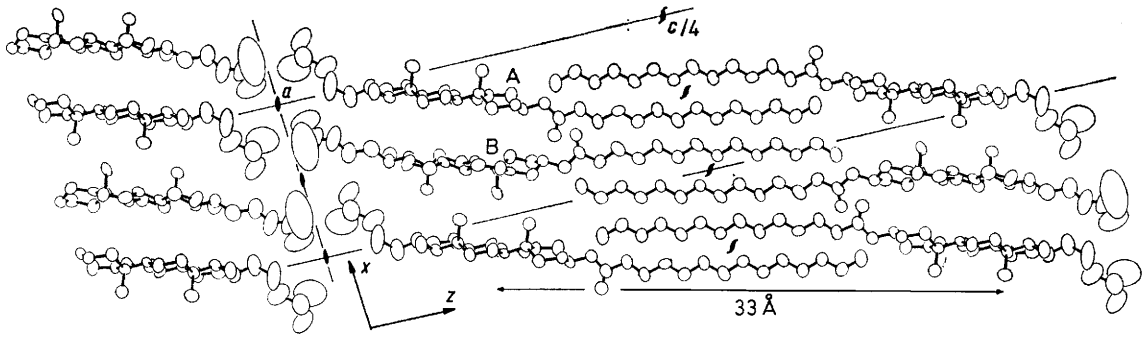

FIGURE 2 Projection of the crystal structure down the *b* axis. Each ellipsoid has 50% probability. The vector of length 33 Å can be translated to give multiple coincidences with its ends at atomic sites

chain atoms (Table 2) is 75° in molecule (B) and 54.5° in molecule (A).

In molecule (B), the chain at C(17) is almost fully extended, but in molecule (A) there is a twist to give a *syn*-conformation about the C(22)–C(23) bond. The torsion angles about C(22)–C(23) are −177.5 and 71.9° in molecules (B) and (A) respectively.

The crystal structure (Figure 2) consists of bilayers of thickness $(d_{001})/2$ or 50.7 Å, in each of which there is an antiparallel arrangement of molecules. Within the bilayer, there is so-called O_a orthorhombic packing [26] of the myristate chains (Figure 4). The orthorhombic substructure has

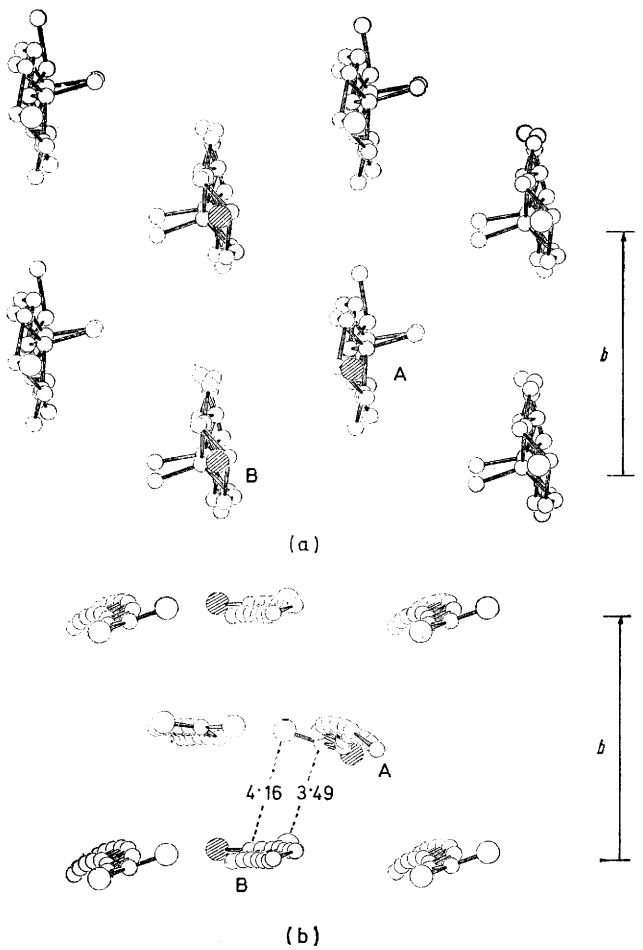

FIGURE 3 Projection of part of the crystal structure down the long axis of the cholesterols. This direction is normal to the *b* axis, making angles 114.4 and 20.0° with the *a* and *c* axes. The molecules marked (A) and (B) are the same as those in Figure 2. The cross-hatched ester oxygen atoms O(3) in Figure 3(a) are superposable on the same atoms in Figure 3(b), so as to join the chains to the cholesterols. (a) The cholesterol fragments C(1)—C(21) from one side of a crystal bilayer. (b) The myristate chains from molecules on both sides of a crystal bilayer. Closest intermolecular carbonyl distances (Å) are shown

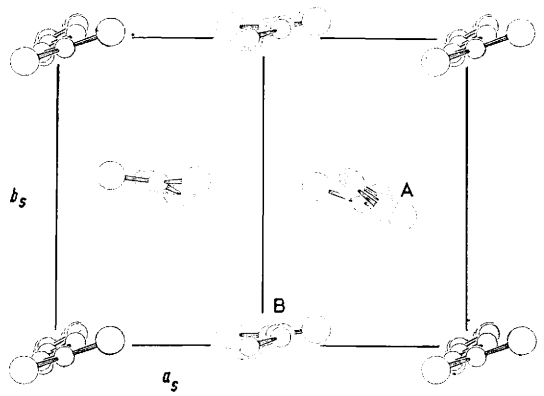

FIGURE 4 The myristate chains, as in Figure 3(b), projected down the c_s axis of the orthorhombic subcell. This axis is normal to the crystal *b* axis and subcell b_s axis (which are identical), and makes angles 110.4 and 16.0° with the crystal *a* and *c* axes

space group *Pnam* and cell dimensions $a_s = 4.9$, $b_s = 7.6$, $c_s = 2.5$ Å with four methylene groups per subcell. The subcell b_s axis is along *b* and c_s is almost along $[\bar{2}01]$. The best least-squares planes through the atoms of the cholesterol rings in molecules (A) and (B) are almost parallel (Table 2), with a dihedral angle of 2°. The normals to these planes make angles of 82 and 81° with the *b* axis. Cholesterol fragments of adjacent (A) and (B) molecules are related by local axes of pseudosymmetry parallel to the length of the molecules (Figures 2 and 3a). The ' symmetry ' operation consists of a 180° rotation followed by a translation of 2.5 Å along the axial direction. Methyl groups C(18) and C(19) then project between neighbouring molecules, while being near to the usual methyl-to-methyl van der Waals distance (4.0 Å) from each other (4.12, 4.13, 4.49, and 4.51 Å). The best least-squares planes passing through the tetracyclic ring systems are unequally spaced. The projecting methyl

[26] E. M. Barrall and J. F. Johnson, in ' Liquid Crystals and Plastic Crystals 2,' eds. G. W. Gray and P. A. Winsor, Wiley, New York, ch. 10; E. Segerman, *Acta Cryst.*, 1965, **19**, 789.

groups cause a greater spacing between adjacent β-faces (5.3 Å) than is observed between the relatively flat α-faces (4.2 Å).

Another noteworthy aspect of the bilayer structure is the close proximity of polar ester groups in neighbouring molecules (Figures 2 and 3b). Carbonyl bonds from molecules (A) and (B) almost overlap in stacking along the *b* direction and are approximately antiparallel with intermolecular C · · · O distances of 3.49 and 4.16 Å. Similar weak carbonyl interactions occur in a variety of other crystal structures.

The efficient packing of the molecules inside the bilayers does not extend to the C(17) chains which form the outer surfaces. Thus, densities calculated for the three different strata within a bilayer are 0.75 for the chains C(20)–C(27) (fractional *z* co-ordinates in the range $0 \lesssim z \lesssim 0.064$), 1.18 for the cholesterol atoms C(1)—(19) ($0.064 \lesssim z \lesssim 0.156$), and 1.02 g cm^{-3} for the myristate chains including ester oxygen atoms ($0.156 \lesssim z \lesssim 0.344$).

DISCUSSION

The low-temperature mesophase of cholesteryl myristate has been classified as smectic A because of its uniaxial behaviour with respect to polarized light, and from miscibility studies of two component systems.[11] Thus it is supposed that the molecular centres are constrained to lie on sheets, with the preferred direction of the long molecular axes orthogonal to the sheets, and with random disorder of molecules within the sheets.

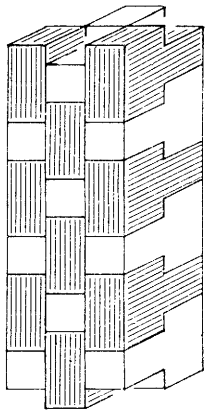

FIGURE 5 Schematic view of a hypothetical layer structure, in which the repeating motif represents a cholesteryl myristate molecule. This pattern differs from the crystal bilayer in that cholesterols are surrounded by myristates and *vice versa*

Wendorff and Price [13] assumed that the inner *X*-ray diffraction ring for smectic and cholesteric cholesteryl myristate arises from a regular stacking of molecular sheets and, from the Bragg equation, obtained an interplanar spacing of 33 Å. They suggested a model in which extended molecules of length 37.4 Å were arranged with adjacent molecules antiparallel so that cholesterols were surrounded by myristate chains and *vice versa*. An interpenetration (4 Å) of molecules from adjacent sheets was invoked so as to account for the 33 Å spacing. The arrangement shown schematically in Figure 5 is consistent with Wendorff and Price's model, except for the regular repetition, which does not occur in the smectic phase. In the crystal structure, the cross-sectional areas of a myristate chain (18.5 Å^2; Figure 4) and a cholesterol (36.6 Å^2; Figure 3a) are almost in the ratio 1 : 2. Also, the lengths of the myristate (19.4 Å) and cholesterol moieties (18.0 Å) are almost equal in the fully extended molecule.[6] The layer in Figure 5 is nearly close-packed, when the repeating motif has these dimensions. However, this space-filling property is progressively lost as the ester chains become either shorter or longer than the cholesterol moiety.

We suggest an alternative model for the structure of the smectic and cholesteric phases from considering the possibilities for progressive disordering of the crystal bilayers (Figure 2). If the smectic transition involved only a shearing at bilayer interfaces, the smectic-phase diffraction pattern would continue to show many of the crystalline powder-diffraction rings, including the low-angle 002, 004 reflections, at values of sin θ/λ 0.010 and 0.020 Å^{-1} or *d* spacings of 50.7 and 25.4 Å. The absence of these rings, coupled with the appearance of a broad liquid-like diffraction ring at *ca.* 0.099 Å^{-1} in sin θ/λ indicates that the phase transition is accompanied by further disordering, including the loss of regular structure within a crystal bilayer. However, we differ from Wendorff and Price in supposing that cholesterols remain surrounded by other cholesterols, and extended myristate chains by other chains, more or less as in the crystal bilayer. An occasional shearing parallel to the length of the molecules, whereby abutting C(18) and C(19) methyl groups slip past each other and re-engage, could lead to molecules aligned nearly normal to the bilayer surface. Rotations about their long axes of molecules or, more likely, of small groups of molecules, could also occur. Such movements, coupled with the liquid-like mobility of the C(17) chains would lead to marked irregularities and curvatures at the bilayer interfaces. These would prevent the regular stacking of bilayers necessary for a characteristic *d* spacing to be observed. We account for the observed inner diffraction ring (sin θ/λ 0.015 Å^{-1}) by assuming that despite the disordering, there is a high probability for each molecule to be paired with an antiparallel close neighbour as in the crystal bilayer. We took the crystal atomic positional and thermal parameters for molecule (A) and a two-fold screw related molecule and calculated the Fourier transform $F(s)F^*(s)$ for the isolated pair as a function of $|s| = \sin\theta/\lambda$ in three-dimensional reciprocal space. This function, which is related to the diffracted intensity, was found to have only one significant peak in the region $|s| < 0.1$ Å^{-1}, other than the origin peak at $|s|$ 0. This peak was quite sharp and strong (5% of the origin peak-height). It occurred in the direction parallel to the long axis of the paired molecules at $|s|$ 0.015 Å^{-1}, in excellent agreement with the radius of the observed inner diffraction ring. We repeated the calculation with a pair of (B) molecules and obtained the same result. From examination of the bilayer structure (Figure 2), we noted multiple interatomic vectors which are nearly parallel and of almost equal length (33 Å) and which run between cholesterol atoms of neighbouring

molecules on opposite sides of the bilayer. These would account for the peak in $F(s)F^*(s)$.*

In the cholesteric phase, the observed weaker intensity of the inner diffraction ring, its increased breadth and shift to $|s|$ 0.016 Å^{-1} are consistent with increased thermal motion of the antiparallel paired molecules. Presumably, this is accompanied by a loss of smectic layering. A decrease in the average separation of paired cholesterols of *ca.* 2 Å is accompanied by increased variability in the molecular arrangement.

Structures of such complexity as the mesophases of cholesteryl myristate cannot be conclusively determined from their *X*-ray diffraction patterns alone. The different models which have been suggested are both consistent with the *X*-ray data. By attributing the inner diffraction ring in both smectic and cholesteric mesophases to the pairing of antiparallel molecules, we must assume that the smectic A layers are not as well defined as is generally believed. On the other hand, if the inner ring for both mesophases is attributed to the regular stacking of well-defined layers, this is contrary to the accepted notion that a cholesteric mesophase has structural similarities to a nematic mesophase, in which the long axes of neighbouring molecules tend to be parallel but the molecules are not organized in layers.† Additional crystallographic studies and a consideration of the physical and chemical properties of related compounds are needed for a better understanding of mesophase structure. In reviewing thermodynamic data for the homologous series of n-acyl cholesteryl esters, Barrall and Johnson [26] suggest that with increasing chain-length, the nonanoate marks the beginning of a new type of order in both crystal and mesophases. The structures of neighbouring homologous esters may well feature the kind of packing arrangement which is observed for the myristate. Possibly, the nonanoate gives the minimum chain-length for which co-operative van der Waals interactions stabilize the close packing of antiparallel alkyl chains.‡

Finally, we point out features in the crystal structure of cholesteryl myristate which may be relevant to the association of cholesterol with the polar lipids of artificial and biological membranes.[2,16] In these membranes, proposed molecular models [27] show cholesterol with the O(3) hydroxy-group in the polar regions of the membranes and with the long molecular axis more or less parallel to surrounding lipid chains. This accounts for the stiffening and closer packing of lipid chains in the presence of cholesterol, presumably inducing a greater degree of local ordering.

In the crystal structure of cholesteryl myristate, the cholesterols are surrounded by other cholesterols, rather than by myristate chains. Nevertheless, the 2 : 1 cross-sectional area relationship discussed earlier, led us to consider the ways in which a group of $2n$ alkyl chains from an orthorhombically packed array might be substituted by a group of n cholesterol molecules, with minimal disturbance of surrounding chains. The orthorhombic chain-packing in cholesteryl myristate is similar to the arrangement in the crystal structure of 1,2-dilauroyl-DL-phosphatidylethanolamine–acetic acid (1 : 1),[28] which provides the only available model of the phospholipid bilayer at atomic resolution. For $n = 1$, we found no satisfactory substitution, but for $n = 2$ we noted that in Figure 3a, molecules (A) and (B) with β-sides in contact give a parallelogram-shaped profile (Figure 6a), resembling that of a group of four alkyl chains (Figure 6c), selected from Figure 4. The superposition (Figure 6b) requires a twisting (15°) of the subcell b_s axis with respect to the crystallographic b axis. Previously suggested models for cholesterol–phospholipid bilayers do not show a pairing of cholesterols.[27]

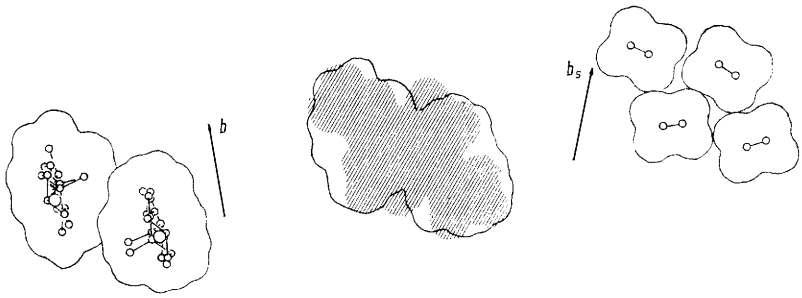

FIGURE 6 Superposition of the profiles of two cholesterol molecules on four myristate chains. The molecular boundaries are drawn at van der Waals radius (1.2 Å) from peripheral hydrogen atoms. The arrangement in (a) is taken from Figure 3(a), that in (c) from Figure 4

* We also calculated $F(s)F^*(s)$ for a pair of antiparallel (A) molecules oriented as in the crystal, but translated so that C(41) and C(27) were opposite each other. This function was effectively zero at $|s|$ 0.015 Å^{-1}, but showed a weak peak at 0.022 Å^{-1} corresponding to a shortening of intermolecular atomic vectors from 33 to 23 Å. Variations of this model could result in non-zero scattered intensity at s 0.015 Å^{-1} and hence be consistent with the structure suggested by Wendorff and Price.

† Cholesteric mesophases also exhibit very long-range ordering with helical characteristics.[4] However, *X*-ray diffraction is insensitive to such structuring.

‡ An extended nonanoate chain would be *ca.* 6 Å shorter than a myristate. The inner diffraction ring for smectic cholesteryl nonanoate [13] corresponds to a d spacing of 27 Å, which is 6 Å shorter than for the myristate. This result is consistent with both suggested structural models for the smectic mesophase.

[27] C. R. Worthington, *Ann. New York Acad. Sci.*, 1972, **195**, 292; D. A. Kirchner and D. L. D. Caspar, *ibid.*, p. 309.
[28] P. B. Hitchcock, R. Mason, K. M. Thomas, and G. G. Shipley, *Proc. Nat. Acad. Sci. U.S.A.*, 1974, **71**, 3036.

However, we suggest that this could be a favourable arrangement, particularly for cholesterol surrounded by alkyl rather than alkenyl phospholipid chains.

Dr. R. Shiono wrote or modified many of the computer programs used, *e.g.*, ORTEP by Dr. C. K. Johnson, used for Figures 1—4. The Laue camera for liquid crystal diffraction was designed and built by Paul Kruth. This work was supported in part by a training grant from the U.S. Public Health Service, National Institutes of Health.

[5/1718 *Received*, 8*th September*, 1975]